Proceedings of the Symposium K: "Complex Oxide Materials for New Technologies"
of E-MRS Fall Meeting 2006, Warsaw, September 4–8, 2006

Layered Cobaltites: Synthesis, Oxygen Nonstoichiometry, Transport and Magnetic Properties

K. Conder[a], A. Podlesnyak[b], E. Pomjakushina[a] and M. Stingaciu[a]

[a]Paul Scherrer Institut (PSI), WLGA, Villigen PSI 5232, Switzerland
[b]Hahn-Meitner-Institut (HMI), Glienicker Str. 100, Berlin 14109, Germany

Complex cobalt oxide perovskite-derived compounds with a general formula $LnBaCo_2O_{5+x}$ (Ln = rare earth) attracted considerable interests because of their interesting properties: magnetic and metal–insulator transitions, giant magnetoresistance, ionic conductivity, and a structural similarity to high temperature superconductors. All the compounds are oxygen nonstoichiometric ($0 < x < 1$) and the cobalt cations can adopt different oxidation and spin states. Compounds with $x \approx 0.5$ display a metal–insulator transition. We found that this transition is affected by an oxygen isotope substitution and is accompanied by structural changes and melting of the orbital ordering. Studies of the metal–insulator transition qualitatively support the models assuming rather carriers delocalization than a spin-state transition in Co^{3+}.

PACS numbers: 72.80.Ga, 71.27.+a, 75.47.De, 61.12.Ld, 71.70.Ej

1. Introduction

Layered cobalt oxide compounds $LnBaCo_2O_{5+x}$ (where Ln — rare earth cation) have a perovskite-derived structure similar to those of high temperature superconductors. The crystal structure of the $LnBaCo_2O_{5+x}$ (Ln112) compounds consists of a sequence of $[CoO_2]$–[BaO]–$[CoO_2]-[LnO_x]$ layers along the c axis (see Fig. 1). Despite not superconducting, these compounds have interesting physical properties (magnetoresistance, metal–insulator transition, ionic conductivity). Layered cobaltites are stable within very wide ranges ($0 \leq x < 1$) of oxygen nonstoichiometry as the cobalt cation can adopt different oxidation states. Depending on the oxygen content the Co-coordination changes from purely pyramidal CoO_5 ($x = 0$) through a coexistence of both pyramidally and CoO_6 octahedrally coordinated cobalt to pure octahedral coordination at $x = 1$. In the intermediate oxidized ($x = 0.5$) Ln112 cobalt cations have an average charge 3+ but exist in

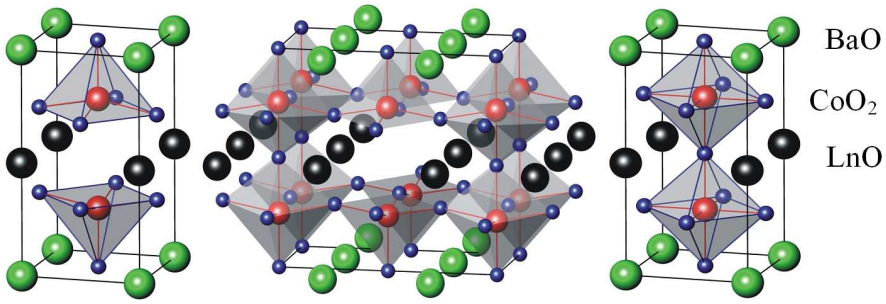

Fig. 1. Schematic crystal structure of $LnBaCo_2O_{5+x}$ with, from left to right, $x = 0$, $x = 0.5$, and $x = 1$.

two coordination pyramidal and octahedral environments. The oxygen vacancies, situated in LnO_x layer, have a strong tendency to order into channels along the a crystallographic direction.

Cobalt cations can exist in different spin states e.g. Co^{3+} ions are diamagnetic in the low-spin (LS) state $t_{2g}^6 e_g^0$ ($S = 0$), while they are paramagnetic in the intermediate-spin (IS) $t_{2g}^5 e_g^1$ and high-spin (HS) $t_{2g}^4 e_g^2$ states with $S = 1$ and 2, respectively. It is believed that spin state transitions can be induced by changing temperature. In addition to that, the compounds with x close to 0.5 display a metal–insulator transition slightly above room temperature [1]. Dependent both on rare-earth cation and oxygen content very rich magnetic phase diagrams are observed for layered cobaltites [2].

2. Synthesis

Polycrystalline samples of $LnBaCo_2O_{5+x}$ are prepared by a solid state reaction using $BaCO_3$ and oxides of cobalt and rare-earth metals. Mixed powders of starting materials in appropriate molar ratios are grounded then pressed into pellets and heated at 1000–1200°C in air with several intermediate grindings. Depending on the rare-earth cation, the oxygen content in as-prepared samples varies from 5.4 (Gd, Ho, Y) to 5.7 (Pr, Nd). Series of samples with different oxygen contents were prepared. For this purpose starting powder material was annealed at elevated oxygen pressure in order to get the highest possible oxygen content. Then, the oxygen content was adjusted by gettering i.e. heating of the known amount of the sample with getter (metallic Y or Cu) in sealed ampoules and slow cooling. Oxygen content was determined by thermogravimetric analysis (hydrogen reduction) and by standard iodometric titration [3]. Single crystal samples have been prepared applying the traveling floating zone method.

3. Metal–insulator transition

Metal–insulator (MI) transition was observed in layered cobaltites for the first time by Martin et al. [1] for both $EuBaCo_2O_{5.4}$ and $GdBaCo_2O_{5.4}$ at

$T_{MI} \approx 360$ K. Above T_{MI} nearly constant resistivity, below clear insulating behaviour and at T_{MI} an increase in resistivity of about one order of magnitude were observed. At temperatures below T_{MI} resistivity of the material can be tuned with magnetic field leading to a giant negative magnetoresistivity (GMR) [1]. In measurements performed for Ln112 (Ln = Pr, Nd, Sm, Eu, Gd, Tb, Dy, and Ho) the MI-transition was always observed at x close to 0.5 [4]. It was found that contrary to the manganates where T_{MI}, T_{MR} (magnetoresistivity peak) and transition from a ferromagnetic to an antiferromagnetic state coincide, in cobaltites T_{MR} is much smaller than T_{MI}. It is still not clear if MI-transition correlates with some magnetic properties of layered perovskites. Many possible scenarios assuming cobalt spin state transitions have been proposed in the literature (see [5] for a review). A selective high-spin state to low-spin state transition (upon cooling) of all the Co^{3+} ions in octahedral environment with remaining of the Co^{3+} in pyramids in intermediate spin state proposed by Frontera et al. [6] is probably the most accepted scenario for the MI transition.

Figure 2 shows resistivity measurements performed on $TbBaCo_2O_{5.5}$ single crystal, parallel to c axis and ab plane. The measurements reveal four transitions: at about $T_{MI} \approx 340$ K which is metal–insulator transition, $T_N \approx 260$ K which is the Néel temperature (peak position of the magnetisation), $T_{SSO} \approx 165$ K (spin state ordering temperature) and $T_R \approx 50$ K, at which probably short-range magnetic ordering of terbium is observed. It is interesting to note that the paramagnetic/ferromagnetic (PM/FM) transition, clearly observed in magnetization measurements, could not be detected in transport studies. No essential anisotropy of the transport properties has been stated. Magnetic field measurements (see the inset in Fig. 2) show that only the Néel temperature is influenced by the magnetic field, especially when measured parallel to the ab plane.

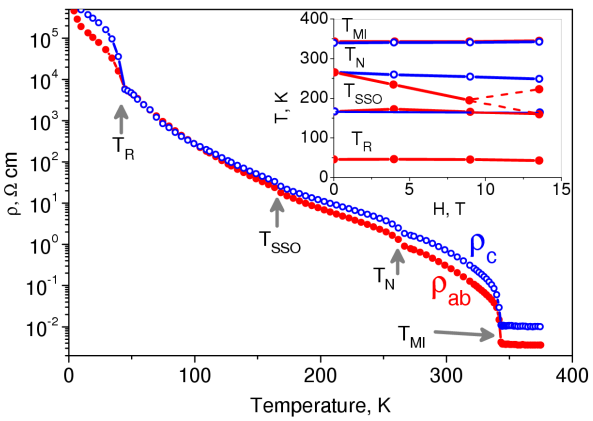

Fig. 2. Temperature dependence of resistivity for single crystal of $TbBaCo_2O_{5.5}$ measured along c (open points) and ab-plane (full points). The inset shows magnetic field dependence of the revealed transition temperatures.

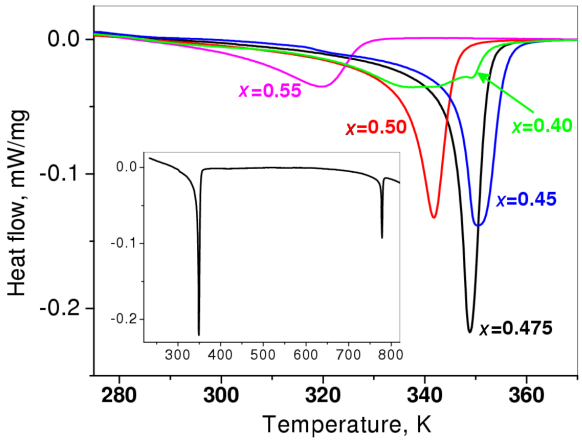

Fig. 3. DSC measurements of metal–insulator transition for $PrBaCo_2O_{5+x}$ samples with different x values. The inset shows the DSC measurements within the whole temperature range 220–820 K. The origin of the high temperature (close to 800 K) transition is discussed in [7].

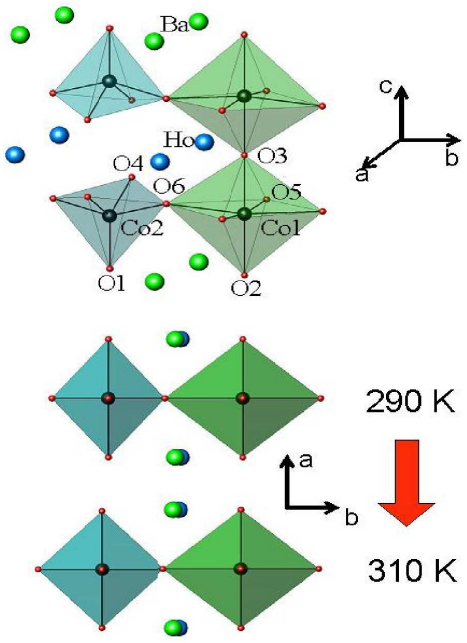

Fig. 4. Schematic crystal structure of $HoBaCo_2O_{5.5}$ at temperatures below (290 K) and above (310 K) the MI transition. The difference in the atomic positions caused by the MI-transition are rescaled to the larger values for better visibility.

The metal–insulator transition manifests itself also by a small change of the magnetic susceptibility, an abrupt change of lattice parameters and bond distances, strong specific heat (c_p) and differential scanning calorimetry (DSC) signals, infrared absorption spectra, and magnetic properties anomalies (see [5] and references therein). DSC is especially sensitive and easy-to-use technique for investigation of the MI-transition. Figure 3 shows the signals obtained for a series of Pr112 samples with different oxygen contents. As it can be seen both heat of MI-transition and peak temperature depend very strongly on oxygen content x.

In order to investigate possible structural transformations across the MI-transition, we have performed high resolution neutron diffraction measurements of the crystal structure in $HoBaCo_2O_{5.5}$ [8]. Figure 4 shows schematically the crystal structure of $HoBaCo_2O_{5.5}$ at temperatures below and above T_{MI}, depicting structural changes observed over the MI-transition. Below T_{MI} both CoO_5-pyramids and CoO_6-octahedra are deformed. Above T_{MI} all the Co2–O bond distances (Co2–O4, Co2–O5, and Co2–O1) become equal and consequently CoO_5-pyramids are not distorted. In the CoO_6-octahedra the bond distances along c-direction i.e. Co1–O2 and Co1–O3 become different in the high-temperature phase whereas in-plane bond lengths (Co1–O6 and Co1–O5) are nearly not affected by the transition. These results suggest an orbital ordering (OO) in the (ab) plane below T_{MI} similar to that proposed previously by Moritomo et al. [9]. The OO expands over all Co ions both in the octahedral (Co1) and pyramidal (Co2) surroundings, i.e. the longest bond length Co1–O6 matches to the shortest Co2–O6. Above T_{MI} the OO in pyramids completely melts giving rise to increased conductivity of the sample.

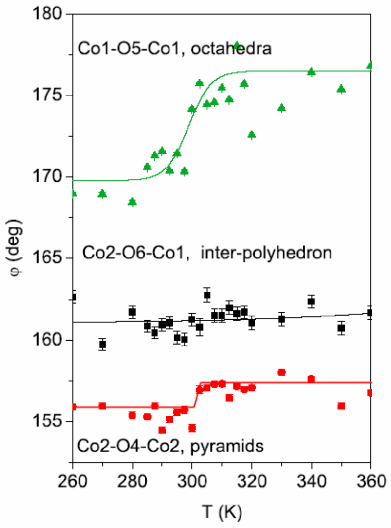

Fig. 5. Temperature dependence of the angles between octahedra Co1–O5–Co1, pyramids Co2–O4–Co2, and inter-polyhedron Co2–O6–Co1 for $HoBaCo_2O_{5.5}$.

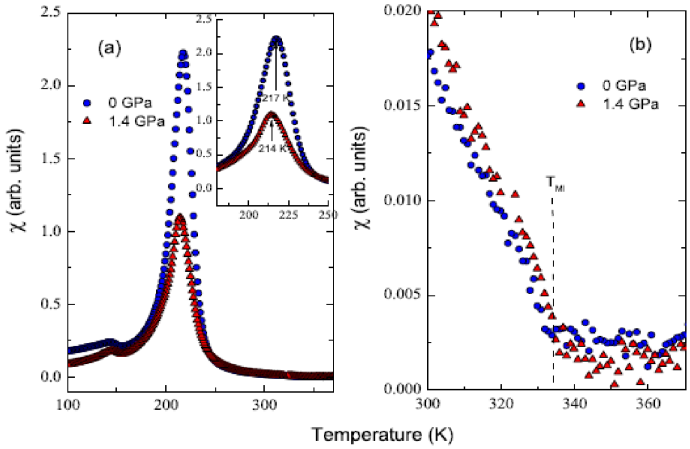

Fig. 6. (a) Temperature dependence of the susceptibility for $PrBaCo_2O_{5.5}$, inset shows susceptibility near the Néel temperature, (b) susceptibility near metal–insulator transition.

The bond lengths of the Co1 in the octahedra do not become equal above T_{MI}. However, the bond angles φ between octahedra Co1–O5–Co1 and between pyramids Co2–O4–Co2 are increased at the transition temperature (Fig. 5), implying that the electron transfer integral through both Co–O–Co, which is proportional to $\cos\varphi$ has a step-like increase, suggesting that the charge carriers delocalization occurs in all directions.

It is known that pressure can modify magnetic and transport properties of transition metal oxides. Pressure induced spin-state and MI-transitions have been reported for many perovskites (see [10] and references therein). Our measurements for $TbBaCo_2O_{5.5}$ [10] and $PrBaCo_2O_{5.5}$ (see Fig. 6) show that the pressure coefficients of the Néel temperatures, as well as T_{MI} are rather small ($\approx$ 2 K/GPa). Applying a pressure favours the LS state since the LS Co^{3+} has a much smaller radius (0.685 Å) than in the HS state (0.75 Å). Therefore, the LS–HS spin-state transition should be shifted to higher temperatures. The effect observed in our experiment is very small suggesting only a weak change of the spin states at the MI transition.

4. Oxygen isotope effect

Differential scanning calorimetry measurements have been performed for selected $LnBaCo_2O_{5+x}$ (Ln = Pr, Dy, Ho, Y) samples substituted with ^{16}O- and ^{18}O-isotopes and oxygen contents close to $5 + x = 5.5$ [11]. Figure 7 shows DSC signals at metal–insulator transition together with a reverse magnetic susceptibility for $HoBaCo_2O_{5.48}$. As it can be seen, ^{18}O-substitution increases the transition temperature T_{MI} but the shift of the T_{MI} is rather small in comparison to that

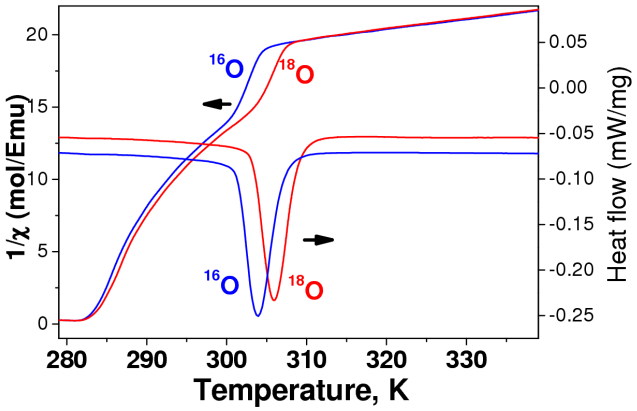

Fig. 7. Inverse magnetic susceptibility and DSC signal for ^{16}O- and ^{18}O-substituted $HoBaCo_2O_{5.48}$ samples.

observed in manganates and nickelates [12, 13]. Measurements of the reverse susceptibility can suggest that a spin state transition can be an origin of the metal–insulator transition. However, a purely magnetic driven transition is not expected to show an isotope effect.

The performed experiments clearly show that the electronic properties of the studied compounds are influenced by the lattice vibrations. According to Jahn–Teller (JT) polaron model, the gap energy $E_g \sim k_B T_{MI}$ of a charge-transfer (CT) insulator can be expressed as a difference between the charge-transfer energy Δ_{CT} and half of the band width W, i.e. $k_B T_{MI} = \Delta_{CT} - W/2$ [12]. JT polaron reduces the band width by means of an exponential renormalization factor $W = W_b \exp(-\gamma E_{JT}/\hbar\omega)$, where E_{JT} is the JT energy and ω is the frequency of the active JT mode. As ω is inversely proportional to $\sqrt{m_0}$, one can expect a rise in T_{MI} by increasing the oxygen isotope mass.

5. Summary

Structural and magnetic properties of layered cobaltites strongly depend on the oxygen concentration. It was found that metal–insulator transition temperature T_{MI} depends neither on magnetic field nor on pressure but shows an oxygen isotope effect.

The results of our studies of the MI transition qualitatively support the models in which the observed transition is associated to hole delocalization in the Co^{3+} high spin state, rather than a spin-state transition.

References

[1] C. Martin, A. Maignan, D. Pelloquin, N. Nguyen, B. Raveau, *Appl. Phys. Lett.* **71**, 1421 (1997).

[2] A. Taskin, A.N. Lavrov, Y. Ando, *Phys. Rev. B* **71**, 134414 (2005).

[3] K. Conder, E. Pomjakushina, A. Soldatov, E. Mitberg, *Mater. Res. Bul.* **40**, 257 (2005).

[4] A. Maignan, C. Martin, D. Pelloquin, N. Nguyen, B. Raveau, *J. Solid State Chem.* **142**, 247 (1999).

[5] A. Podlesnyak, K. Conder, E. Pomjakushina, A. Mirmelstein, in: *Frontal Semiconductor Research*, Ed. O.T. Chang, Nova Science Publishers, Hauppauge (NY) 2006.

[6] C. Frontera, J.L. García-Muñoz, A. Llobet, M.A.G. Aranda, *Phys. Rev. B* **65**, R180404 (2002).

[7] S. Streule, A. Podlesnyak, E. Pomjakushina, K. Conder, D. Sheptyakov, M. Medarde, J. Mesot, *Physica B* **378-380**, 539 (2006).

[8] E. Pomjakushina, K. Conder, V. Pomjakushin, *Phys. Rev. B* **73**, 094203 (2006).

[9] Y. Moritomo, T. Akimoto, M. Takeo, A. Machida, E. Nishibori, M. Takata, M. Sakata, K. Ohoyama, A. Nakamura, *Phys. Rev. B* **61**, R13325 (2000).

[10] A. Podlesnyak, S. Streule, K. Conder, E. Pomjakushina, J. Mesot, A. Mirmelstein, P. Schützendorf, R. Lengsdorf, M.M. Abd-Elmeguid, *Physica B* **378-380**, 537 (2006).

[11] K. Conder, E. Pomjakushina, V. Pomjakushin, M. Stingaciu, S. Streule, A. Podlesnyak, *J Phys., Condens. Matter.* **17**, 5813 (2005).

[12] Zhao Guo-meng, K. Conder, H. Keller, K.A. Müller, *Nature* **381**, 676 (1996).

[13] M. Medarde, P. Lacorre, K. Conder, F. Fauth, A. Furrer, *Phys. Rev. Lett.* **80**, 2397 (1998).